

## Electronic Supplementary Information (ESI)

# Single-Ion Magnets based on Mononuclear Lanthanide Complexes with Chiral Schiff base Ligand [Ln(FTA)<sub>3</sub>L] (Ln= Sm, Eu, Gd, Tb and Dy)

Dong-Ping Li, Tian-Wei Wang, Cheng-Hui Li\*, Dong-Sheng Liu, Yi-Zhi Li, Xiao-Zeng You\*

*State Key Laboratory of Coordination Chemistry, School of Chemistry and Chemical Engineering, Nanjing National Laboratory of Microstructures, Nanjing University, Nanjing 210093, P. R. China.*

## Experimental details

### Synthesis

All reagents were purchased from commercial suppliers (Aldrich) and used as received. The rare-earth  $\beta$ -diketone complexes dihydrate Ln(FTA)<sub>3</sub>·2H<sub>2</sub>O (Ln = Eu, Nd, Sm, Gd, Tb and Dy) were synthesized by published methods (see main text).

**Dy(FTA)<sub>3</sub>L (1):** An ethanol solution (5 ml) of Eu(TTA)<sub>3</sub>·2H<sub>2</sub>O (0.05 mmol) was added to a solution of L (0.05 mmol) in 5 ml of tetrahydrofuran under stirring. The resultant solution was filtered and placed undisturbed for several days. Block crystal of **1** were obtained in 30% yield, Anal Calc for C<sub>44</sub>H<sub>32</sub>DyF<sub>9</sub>N<sub>2</sub>O<sub>11</sub>: C, 48.12; H, 2.94; N, 2.55%. Found: C, 48.10; H, 3.01; N, 2.54%. Yield: 40%. IR (KBr/cm<sup>-1</sup>): 3415, 1616, 1573, 1522, 1458, 1387, 1309, 1259, 1192, 1136, 671.

The complexes **2–5** were prepared as similar as that of **1** using the respective rare-earth  $\beta$ -diketone dihydrates.

### X-ray crystallography.

Single-crystal X-ray diffraction measurements of complexes **1–5** were carried out on a Bruker SMART APEX CCD diffractometer operating at room temperature. Intensities were collected with graphite monochromatized Mo K $\alpha$  radiation ( $\lambda = 0.71073 \text{ \AA}$ ), using  $\varphi$ - $\omega$  scanning mode. Data integration and empirical absorption corrections were carried out by using SAINT program. The structures were solved by direct method (SHELXS 97). All the non-hydrogen atoms were refined anisotropically based on the  $F^2$  values by

full-matrix least-squares techniques (SHELXL 97). Hydrogen atoms bonded to the carbon atoms were generated geometrically and refined isotropically using the riding mode. The hydrogen atoms of the water molecules atoms were located in the different Fourier maps. Details of the crystal parameters, data collection and refinements for **1** and **2** are summarized in Table 2. CCDC: 752491–752493 and 752495–752496 contains the supplementary crystallographic data for complex **1–5**. These data can be obtained free of charge from the Cambridge Crystallographic Data Centre via [www.ccdc.cam.ac.uk/data\\_request/cif](http://www.ccdc.cam.ac.uk/data_request/cif).

### Physical property measurements

Elemental analyses of all complexes were performed on a Perkin-Elmer 240C analyzer. Infrared spectra were recorded in KBr pellet on a vector22 Bruker spectrophotometer in the range of 400-4000 cm<sup>-1</sup>. The CD spectra were recorded on a JASCO J-810 spectropolarimeter. Electric hysteresis loops were recorded on a Ferroelectric Tester Precision Premier II made by Radiant Technologies, Inc. Variable-temperature magnetic susceptibility, zero-field ac magnetic susceptibility measurements, and field dependence of magnetization on polycrystalline samples were performed on a Quantum Design MPMS-XL7 SQUID magnetometer.

**Table S1.** Crystal Data and Structure Refinements for Complexes **1–5**

Complexes	<b>1</b>	<b>2</b>	<b>3</b>	<b>4</b>	<b>5</b>
Empirical formula	C <sub>44</sub> H <sub>32</sub> F <sub>9</sub> DyN <sub>2</sub> O <sub>11</sub>	C <sub>44</sub> H <sub>32</sub> F <sub>9</sub> SmN <sub>2</sub> O <sub>11</sub>	C <sub>44</sub> H <sub>32</sub> F <sub>9</sub> EuN <sub>2</sub> O <sub>11</sub>	C <sub>44</sub> H <sub>32</sub> F <sub>9</sub> GdN <sub>2</sub> O <sub>11</sub>	C <sub>44</sub> H <sub>32</sub> F <sub>9</sub> TbN <sub>2</sub> O <sub>11</sub>
Formula weight	1098.22	1086.08	1087.68	1092.97	1094.64
Crystal system	trigonal	trigonal	trigonal	trigonal	trigonal
Space group	<i>P</i> 3 <sub>2</sub>				
<i>a</i> (Å)	10.4545(8)	10.4701(10)	10.4826(10)	10.4887(10)	10.4758(16)
<i>b</i> (Å)	10.4545(8)	10.4701(10)	10.4826(10)	10.4887(10)	10.4758(16)
<i>c</i> (Å)	34.431(4)	34.531(6)	34.508(6)	34.490(4)	34.546(7)
$\alpha$ (°)	90.00	90.00	90.00	90.00	90.00
$\beta$ (°)	90.00	90.00	90.00	90.00	90.00
$\gamma$ (°)	120.00	120.00	120.00	120.00	120.00
<i>V</i> (Å <sup>3</sup> )	3259.0(5)	3278.3(7)	3283.8(8)	3286.0(6)	3283.2(10)
<i>Z</i>	3	3	3	3	3
$\theta$ range [ ° ]	2.25 to 25.99	2.25 to 26.00	1.77 to 26.00	1.77 to 25.34	2.24 to 25.98
Collected reflections	17610	17683	24232	16945	17671
Unique	8415	7818	7985	7504	5850
<i>R</i> <sub>int</sub>	0.0437	0.0506	0.0676	0.0541	0.0669
Refined data [ $>2\sigma$ (I)]	6284	6204	6626	6064	4813
<i>T</i> (K)	291(2)	291(2)	291(2)	291(2)	291(2)
<i>R</i> <sub>1</sub> <sup>[a]</sup> , w <i>R</i> <sub>2</sub> <sup>[b]</sup> [ <i>I</i> > 2 $\sigma$ (I)]	0.0497, 0.1084	0.0704, 0.1139	0.0512, 0.1076	0.0492, 0.1026	0.0497, 0.1046
Data/ restraints/para	8415/1/604	7818/1/604	7985/1/604	7504/1/580	5850/1/604
GOF	0.845	1.073	1.084	1.062	0.999

<sup>a</sup>  $R$ 1 =  $\Sigma(|Fo| - |Fc|) / \Sigma|Fo|$ ,  $wR$ 2 =  $[\sum w(|Fo| - |Fc|)^2 / \sum w|Fo|^2]^{1/2}$ .

**Table S2.** Selected Bond Lengths ( $\text{\AA}$ ) and Angles ( $^\circ$ ) for **1–5**

Complex 1			
Dy(1)–O(3)	2.248(5)	Dy(1)–O(1)	2.286(5)
Dy(1)–O(2)	2.274(6)	Dy(1)–O(5)	2.320(6)
Dy(1)–O(4)	2.401(5)	Dy(1)–O(6)	2.408(6)
Dy(1)–N(1)	2.584(7)	Dy(1)–N(2)	2.580(6)
O(3)–Dy(1)–O(1)	85.3(2)	O(3)–Dy(1)–O(2)	148.5(2)
O(1)–Dy(1)–O(2)	74.5(2)	O(3)–Dy(1)–O(5)	107.3(2)
O(1)–Dy(1)–O(5)	144.6(2)	N(1)–Dy(1)–N(2)	64.0(2)
O(1)–Dy(1)–N(2)	95.9(2)	O(6)–Dy(1)–N(2)	69.9(2)
O(3)–Dy(1)–N(2)	135.9(2)	O(4)–Dy(1)–N(2)	151.6(2)
O(6)–Dy(1)–N(1)	69.9(2)	O(5)–Dy(1)–N(2)	97.0(2)
O(2)–Dy(1)–O(5)	78.7(2)	O(2)–Dy(1)–N(2)	71.3(2)
O(4)–Dy(1)–N(1)	138.4(2)	O(2)–Dy(1)–N(1)	122.0(2)
O(5)–Dy(1)–N(1)	139.6(2)	O(4)–Dy(1)–O(6)	128.2(2)
O(1)–Dy(1)–N(1)	75.4(2)	O(5)–Dy(1)–O(6)	70.0(2)
O(3)–Dy(1)–N(1)	73.8(2)	O(1)–Dy(1)–O(6)	145.3(2)
O(2)–Dy(1)–O(6)	125.7(2)	O(3)–Dy(1)–O(6)	84.3(2)
O(5)–Dy(1)–O(4)	74.2 (2)	O(2)–Dy(1)–O(4)	80.4(2)
O(3)–Dy(1)–O(4)	72.0(2)	O(1)–Dy(1)–O(4)	78.9(2)
Complex 2			
Sm(1)–O(3)	2.322(6)	Sm(1)–O(1)	2.340(6)
Sm(1)–O(2)	2.345(6)	Sm(1)–O(5)	2.356(6)
Sm(1)–O(4)	2.418(5)	Sm(1)–O(6)	2.431(6)
Sm(1)–N(1)	2.634(6)	Sm(1)–N(2)	2.654(7)
O(3)–Sm(1)–O(1)	85.9(2)	O(3)–Sm(1)–O(2)	147.2(2)
O(1)–Sm(1)–O(2)	72.5(2)	O(1)–Sm(1)–O(6)	145.9(2)
O(3)–Sm(1)–O(5)	108.5(2)	O(1)–Sm(1)–O(5)	144.1(2)
O(2)–Sm(1)–O(5)	78.8(2)	O(3)–Sm(1)–O(4)	71.9(2)
O(1)–Sm(1)–O(4)	79.5(2)	O(2)–Sm(1)–O(4)	80.0(2)
O(5)–Sm(1)–O(4)	74.5(2)	O(3)–Sm(1)–O(6)	84.8(2)
O(2)–Sm(1)–O(6)	126.7(2)	O(5)–Sm(1)–O(6)	69.7(2)
N(1)–Sm(1)–N(2)	63.5(2)	O(6)–Sm(1)–N(2)	71.5(2)
O(4)–Sm(1)–N(2)	150.8(2)	O(5)–Sm(1)–N(2)	96.9(2)
O(2)–Sm(1)–N(2)	70.9(2)	O(1)–Sm(1)–N(2)	93.7(2)
O(3)–Sm(1)–N(2)	136.5(2)	O(6)–Sm(1)–N(1)	70.1(2)
O(4)–Sm(1)–N(1)	139.2(2)	O(5)–Sm(1)–N(1)	139.1(2)
O(2)–Sm(1)–N(1)	121.5(2)	O(1)–Sm(1)–N(1)	75.8(2)
O(3)–Sm(1)–N(1)	74.4(2)	O(4)–Sm(1)–O(6)	127.7(2)
Complex 3			
Eu(1)–O(7)	2.306(5)	Eu(1)–O(5)	2.320(5)
Eu(1)–N(2)	2.662(6)	Eu(1)–N(1)	2.651(6)
Eu(1)–O(8)	2.427(4)	Eu(1)–O(4)	2.408(5)
Eu(1)–O(1)	2.355(5)	Eu(1)–O(2)	2.310(5)
O(7)–Eu(1)–O(5)	107.4(2)	O(7)–Eu(1)–O(2)	148.8(2)
N(1)–Eu(1)–N(2)	63.0(2)	O(8)–Eu(1)–N(2)	151.5(2)

O(4)—Eu(1)—N(2)	71.1(2)	O(1)—Eu(1)—N(2)	94.4(2)
O(2)—Eu(1)—N(2)	71.0(2)	O(5)—Eu(1)—N(2)	97.2(2)
O(7)—Eu(1)—N(2)	136.2(2)	O(8)—Eu(1)—N(1)	139.4(2)
O(4)—Eu(1)—N(1)	68.7(2)	O(1)—Eu(1)—N(1)	75.9(2)
O(2)—Eu(1)—N(1)	122.2(2)	O(5)—Eu(1)—N(1)	138.9(2)
O(7)—Eu(1)—N(1)	74.9(2)	O(4)—Eu(1)—O(8)	128.0(2)
O(1)—Eu(1)—O(8)	79.5(2)	O(2)—Eu(1)—O(8)	80.6(2)
O(5)—Eu(1)—O(8)	74.4(2)	O(7)—Eu(1)—O(8)	71.6(2)
O(1)—Eu(1)—O(4)	144.6(2)	O(2)—Eu(1)—O(4)	126.0(2)
O(5)—Eu(1)—O(4)	70.8(2)	O(7)—Eu(1)—O(4)	83.4(2)
O(2)—Eu(1)—O(1)	74.8(2)	O(5)—Eu(1)—O(1)	144.4(2)
O(7)—Eu(1)—O(1)	86.3(2)	O(5)—Eu(1)—O(2)	77.4(2)
Complex 4			
Gd(1)—O(1)	2.301(6)	Gd(1)—O(8)	2.326(5)
Gd(1)—O(7)	2.342(5)	Gd(1)—O(5)	2.359(5)
Gd(1)—O(4)	2.389(6)	Gd(1)—O(2)	2.381(5)
Gd(1)—N(1)	2.608(7)	Gd(1)—N(2)	2.625(6)
O(1)—Gd(1)—O(8)	85.4(2)	O(1)—Gd(1)—O(7)	148.0(2)
O(8)—Gd(1)—O(7)	73.9(2)	O(1)—Gd(1)—O(5)	107.6(2)
O(8)—Gd(1)—O(5)	143.4(2)	O(7)—Gd(1)—O(5)	78.2(2)
O(1)—Gd(1)—O(4)	84.3(2)	O(8)—Gd(1)—O(4)	145.5(2)
O(7)—Gd(1)—O(4)	126.2(2)	O(5)—Gd(1)—O(4)	71.0(2)
O(1)—Gd(1)—O(2)	71.7(2)	O(8)—Gd(1)—O(2)	78.6(2)
O(7)—Gd(1)—O(2)	80.3(2)	O(5)—Gd(1)—O(2)	73.7(2)
N(1)—Gd(1)—N(2)	63.7(2)	O(2)—Gd(1)—N(2)	150.9(2)
O(4)—Gd(1)—N(2)	71.4(2)	O(5)—Gd(1)—N(2)	98.0(2)
O(7)—Gd(1)—N(2)	70.6(2)	O(8)—Gd(1)—N(2)	94.7(2)
O(1)—Gd(1)—N(2)	136.5(2)	O(2)—Gd(1)—N(1)	138.6(2)
O(4)—Gd(1)—N(1)	70.0(2)	O(5)—Gd(1)—N(1)	140.5(2)
O(7)—Gd(1)—N(1)	121.6(2)	O(8)—Gd(1)—N(1)	75.6(2)
O(1)—Gd(1)—N(1)	74.4(2)	O(4)—Gd(1)—O(2)	128.2(2)
Complex 5			
Tb(1)—O(1)	2.274(7)	Tb(1)—O(4)	2.296(6)
Tb(1)—O(2)	2.291(7)	Tb(1)—O(7)	2.344(8)
Tb(1)—O(5)	2.411(6)	Tb(1)—O(8)	2.416(8)
Tb(1)—N(1)	2.578(9)	Tb(1)—N(2)	2.628(8)
O(1)—Tb(1)—O(4)	86.1(3)	O(1)—Tb(1)—O(2)	73.9(3)
O(4)—Tb(1)—O(2)	147.7(2)	O(1)—Tb(1)—O(7)	144.3(2)
O(4)—Tb(1)—O(7)	107.2(3)	O(2)—Tb(1)—O(7)	78.2(3)
N(1)—Tb(1)—N(2)	64.8(3)	O(8)—Tb(1)—N(2)	71.1(3)
O(5)—Tb(1)—N(2)	150.0(2)	O(7)—Tb(1)—N(2)	96.0(3)
O(2)—Tb(1)—N(2)	70.4(2)	O(4)—Tb(1)—N(2)	137.8(3)
O(1)—Tb(1)—N(2)	95.2(3)	O(8)—Tb(1)—N(1)	69.4(2)
O(5)—Tb(1)—N(1)	139.3(3)	O(7)—Tb(1)—N(1)	139.3(2)
O(2)—Tb(1)—N(1)	122.1(3)	O(4)—Tb(1)—N(1)	74.9(3)
O(1)—Tb(1)—N(1)	75.7(2)	O(5)—Tb(1)—O(8)	128.0(2)

O(7)–Tb(1)–O(8)	70.4(2)	O(2)–Tb(1)–O(8)	126.5(3)
O(4)–Tb(1)–O(8)	84.0(3)	O(1)–Tb(1)–O(8)	145.1(2)
O(7)–Tb(1)–O(5)	74.0(2)	O(2)–Tb(1)–O(5)	79.8(2)
O(4)–Tb(1)–O(5)	71.7(2)	O(1)–Tb(1)–O(5)	79.4(2)

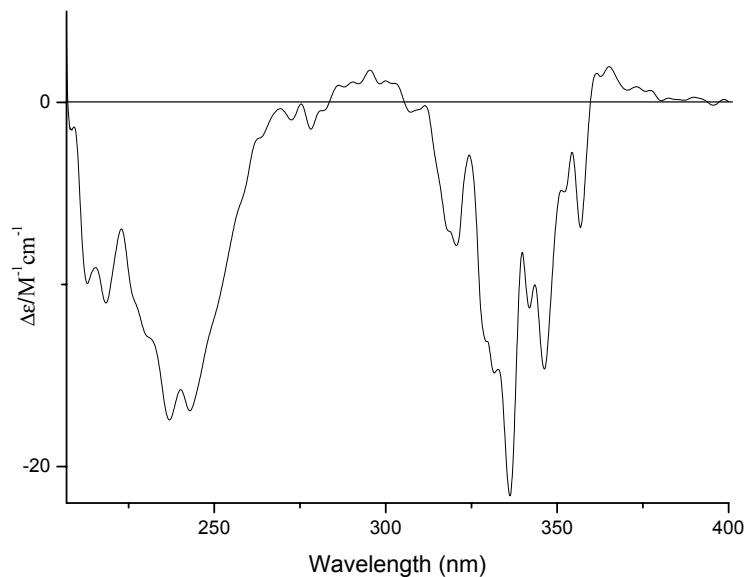


**Figure S1.** Circular dichroism spectrum of **1** in THF.

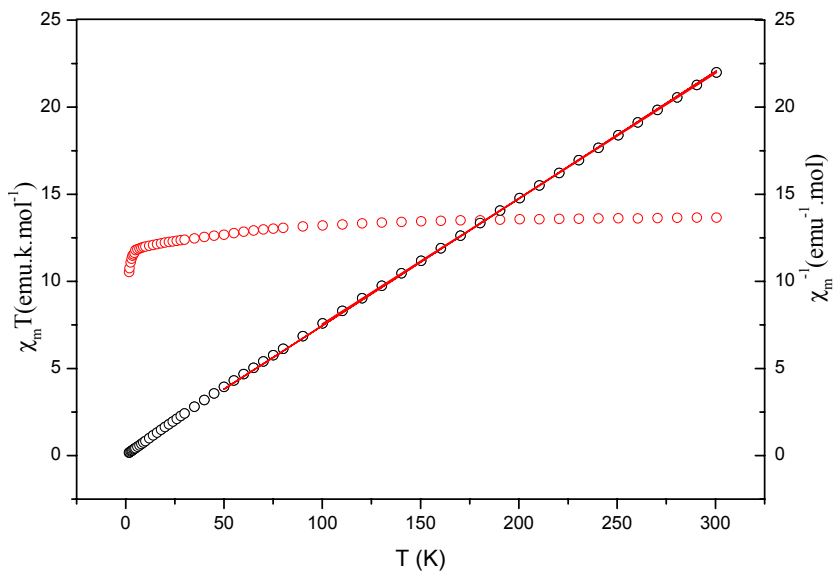


**Figure S2.**  $\chi_M T$ (left) product and  $\chi_M^{-1}$ (right) temperature of **1** at 1.8–300 K. The red line represents the best fitting to Curie-Weiss law in high temperature region.

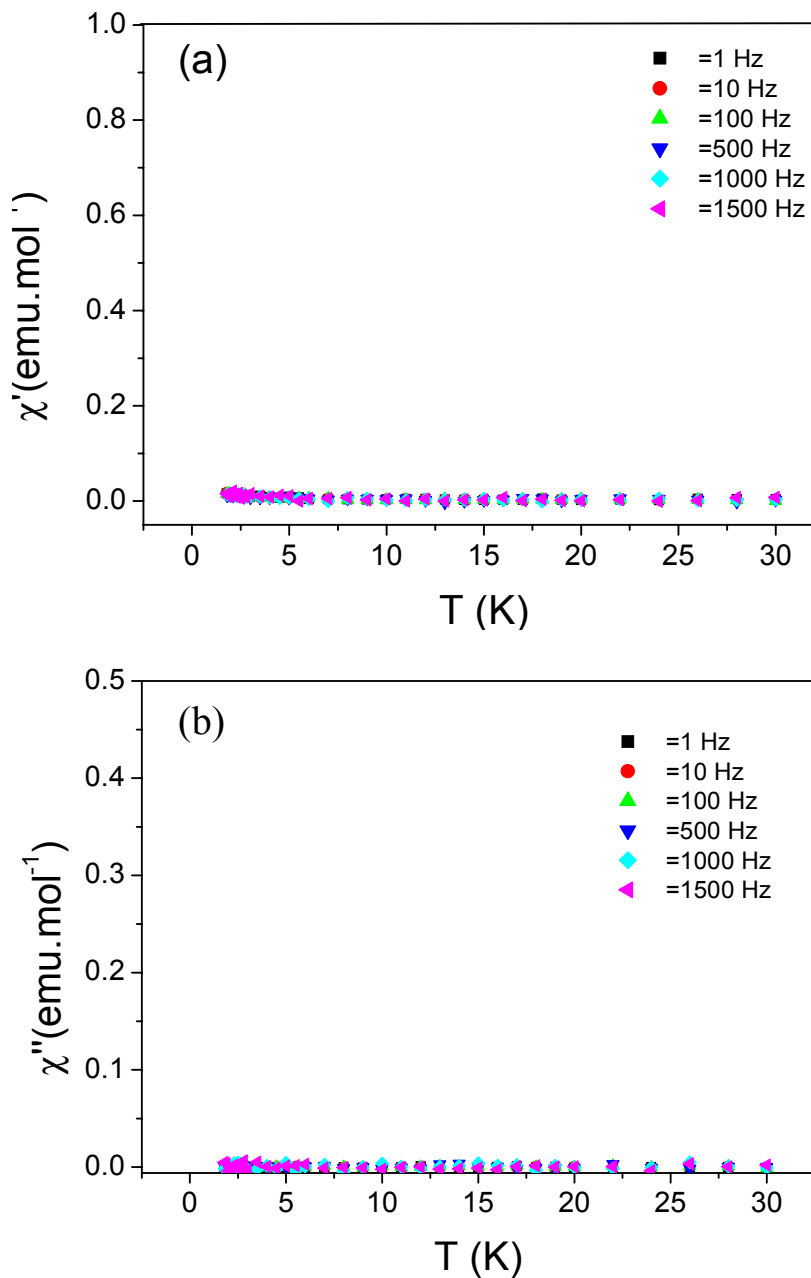


**Figure S3.** (a) Low-frequency In-phase dynamic susceptibility of  $\text{Sm}(\text{FTA})_3\text{L}$ . (b) Low-frequency out-of-phase dynamic susceptibility of  $\text{Sm}(\text{FTA})_3\text{L}$ .

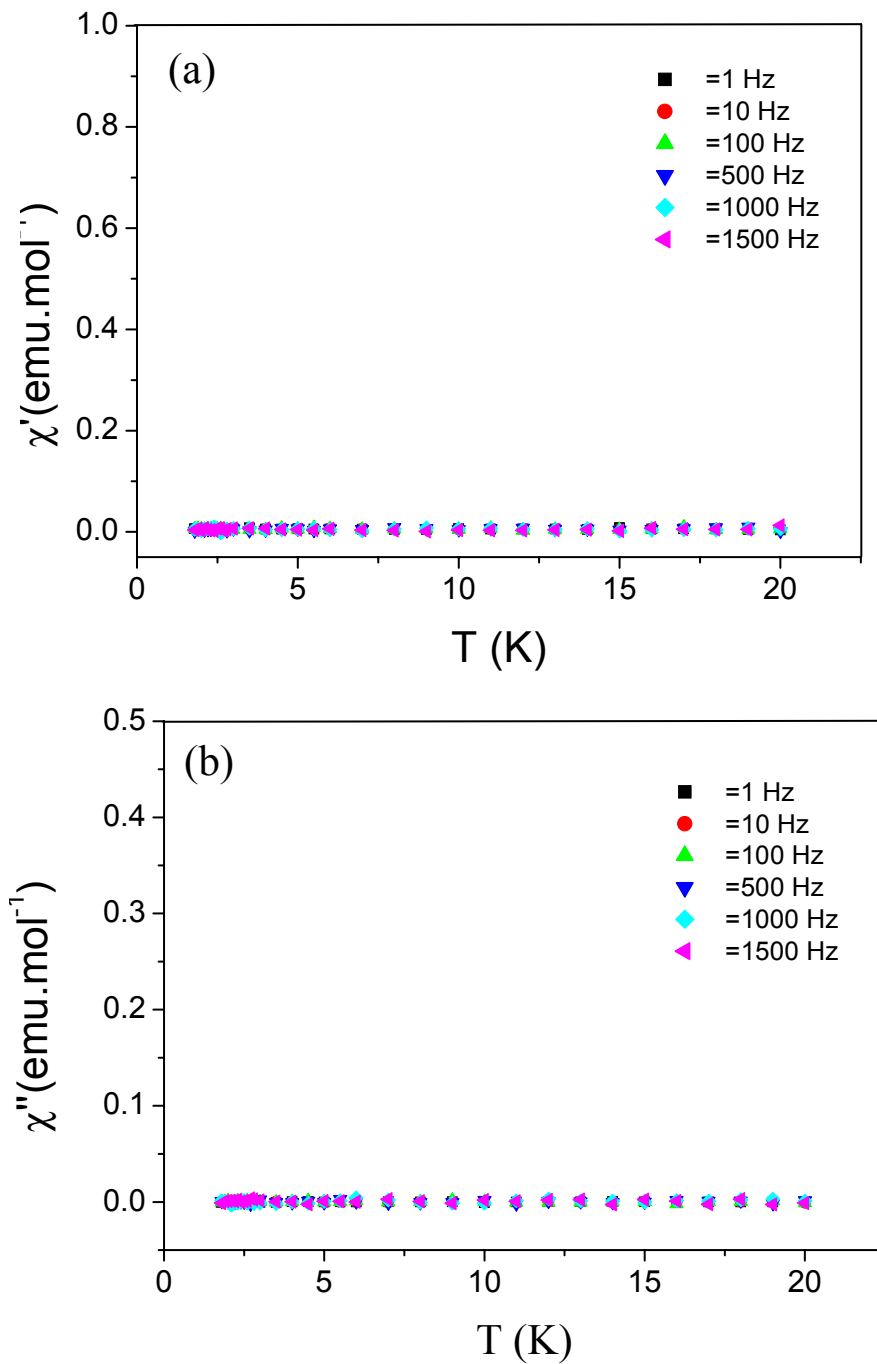


**Figure S4.** (a) Low-frequency In-phase dynamic susceptibility of Eu(FTA)<sub>3</sub>L. (b) Low-frequency out-of-phase dynamic susceptibility of Eu(FTA)<sub>3</sub>L.

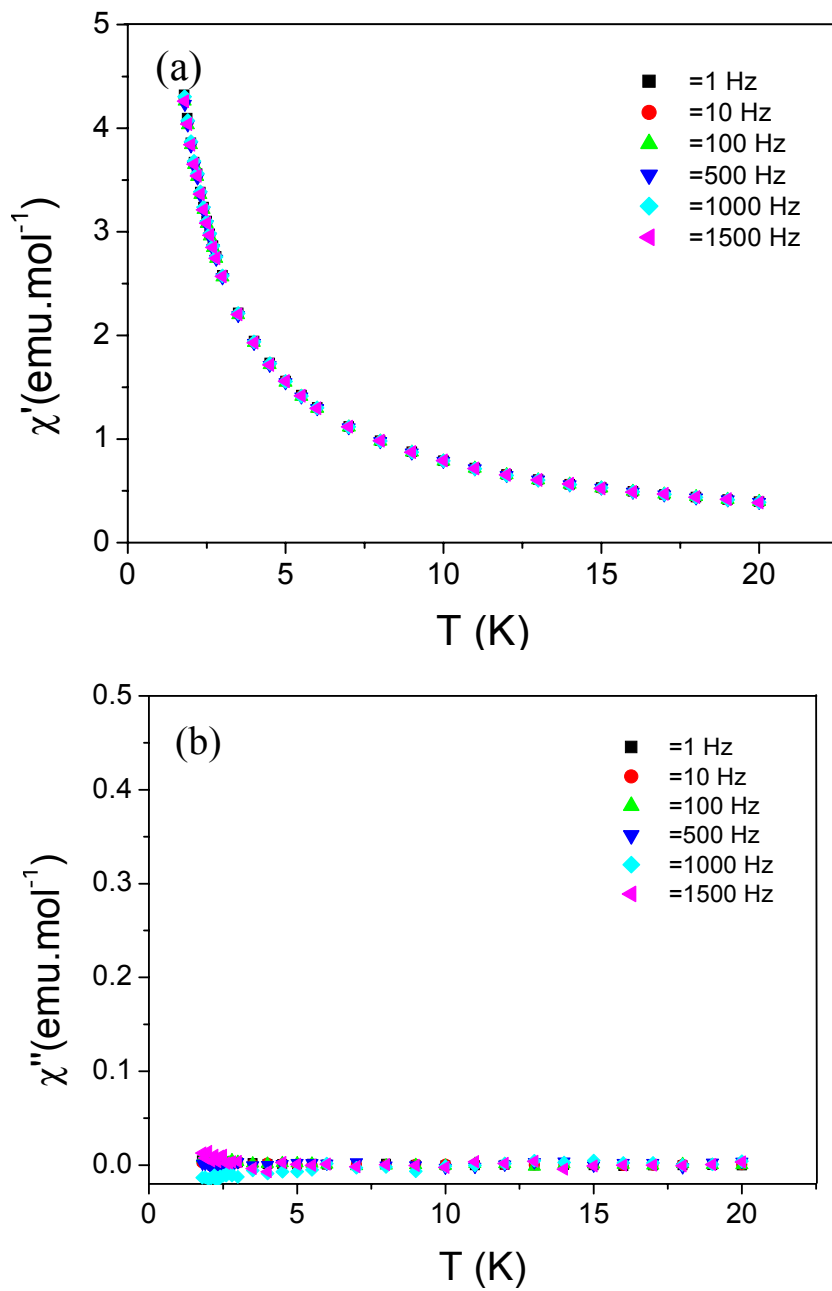


**Figure S5.** (a) Low-frequency In-phase dynamic susceptibility of  $\text{Gd}(\text{FTA})_3\text{L}$ . (b) Low-frequency out-of-phase dynamic susceptibility of  $\text{Gd}(\text{FTA})_3\text{L}$ .

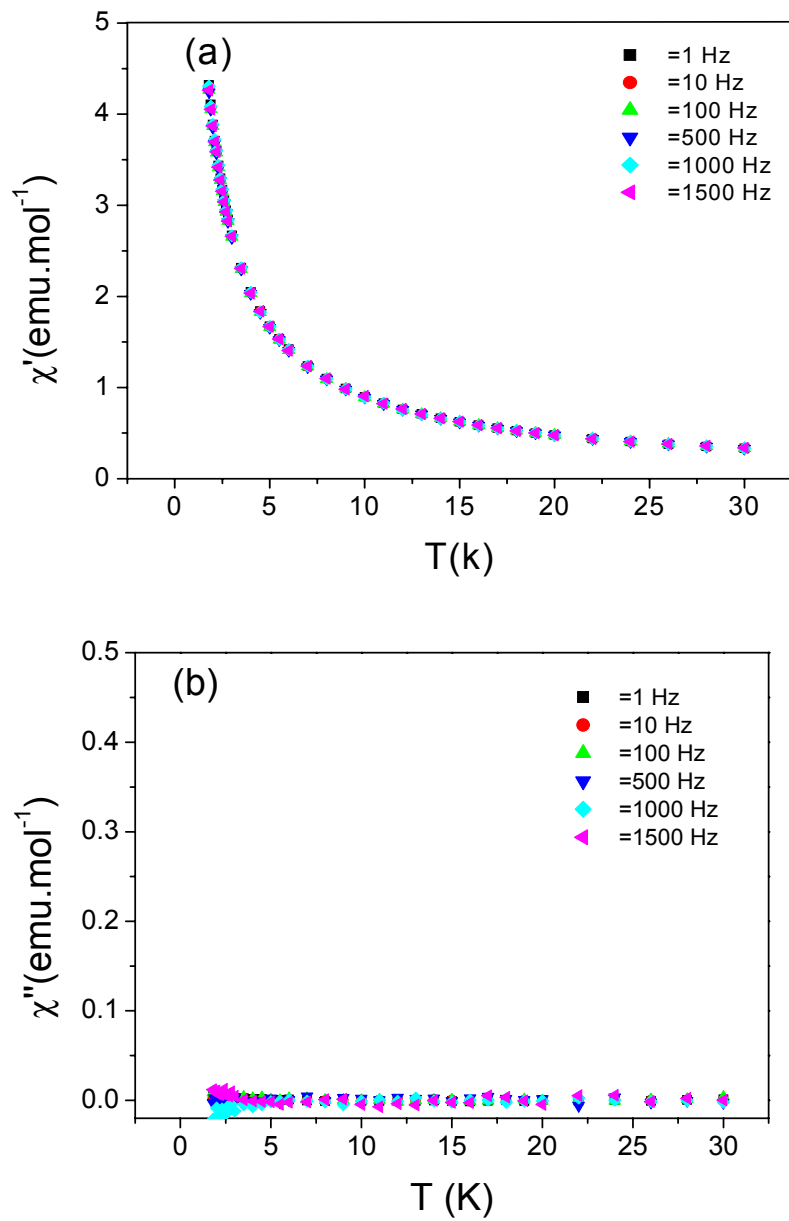


**Figure S6.** (a) Low-frequency In-phase dynamic susceptibility of  $\text{Tb}(\text{FTA})_3\text{L}$ . (b) Low-frequency out-of-phase dynamic susceptibility of  $\text{Tb}(\text{FTA})_3\text{L}$ .

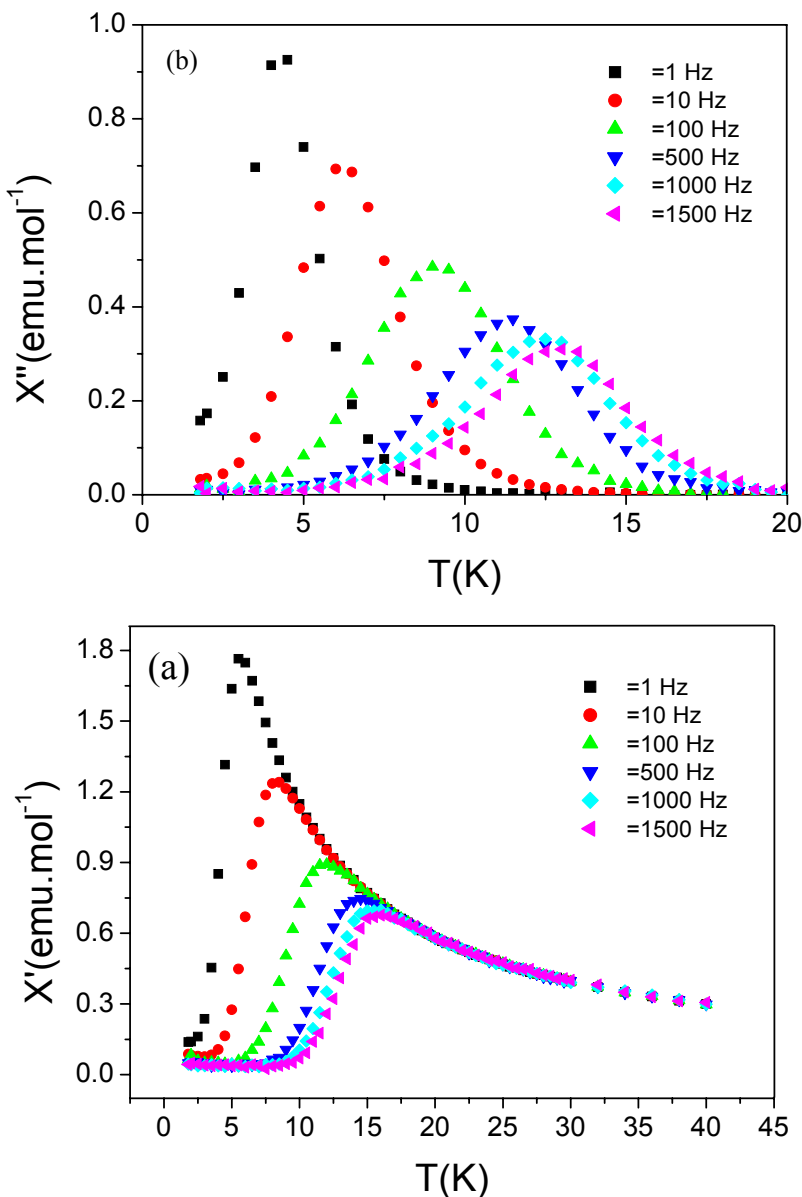


**Figure S7.** (a) In-phase dynamic susceptibility of **1**. (b) out-of-phase dynamic susceptibility of **1** measured in an ac magnetic field of 3 Oe and a dc field of 2000 Oe.

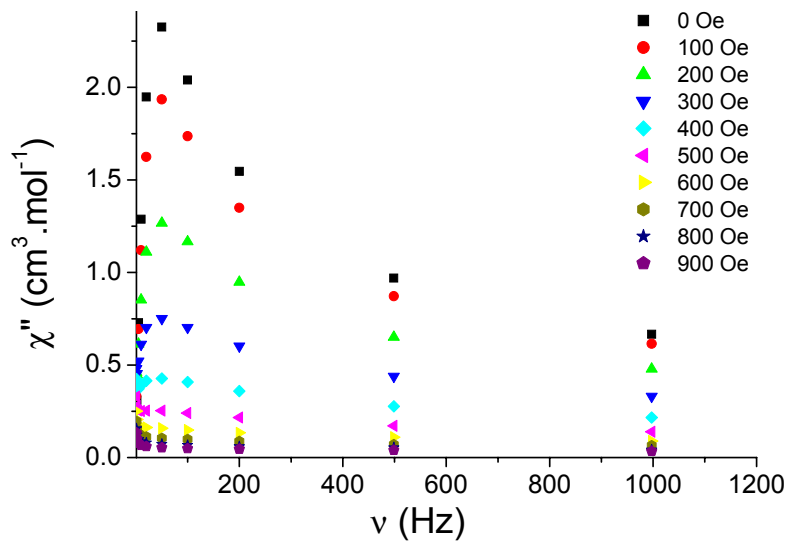


**Figure S8.** Frequency dependence of  $\chi''$  of **1** at different dc magnetic fields. All measurements are performed at 1.8 K.

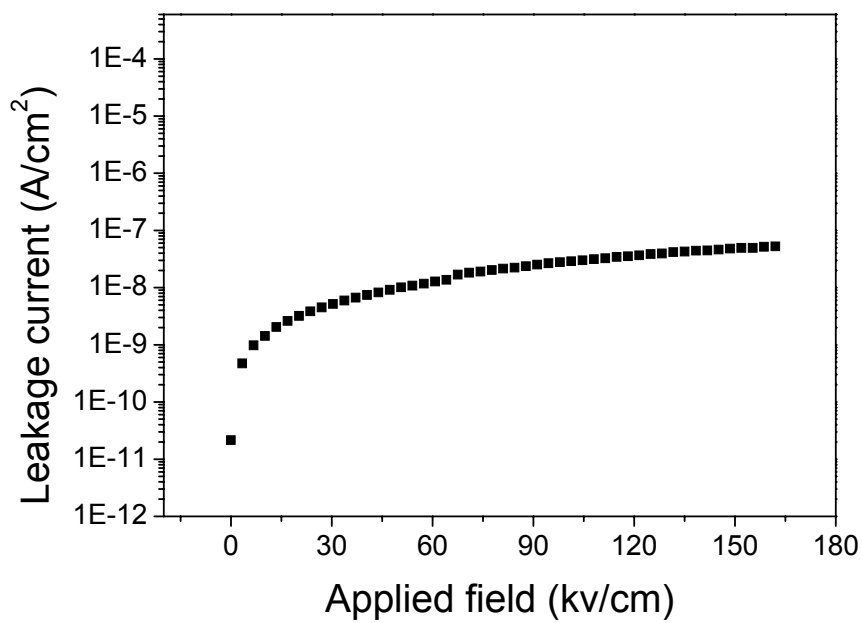


**Figure S9.** Leakage current of ferroelectric hysteresis loop of **1**